UTERINE CONTRACTION CHARACTERISATION DURING LABOUR WITH SMART WIRELESS ECG DETECTION

Dr. Walid A. Zgallai
Faculty of Engineering Technology and Science
HCT
Dubai, UAE
Walidzgallai@yahoo.co.uk

***Abstract*— The aim of this paper is to separate the Uterine Contractions Interference Signal (UCIS) from the combined fetal and mother transabdominal ECG signals. The UCIS is measured during peak contractions at the full-term, 40 weeks of gestation, with a separation of 10 minutes between contractions and 90 seconds in duration. The UCIS signal is then characterized and its eigenvectors are separated into orthogonal subspace to that of the eigenvectors of the fetal and mother components. This improves the detection of fetal and mother spectral peaks uniquely identified from the transabdominally-measured signal by employing adaptive LMS- and LMF-based Volterra filters, higher order statistics, and spectral super-resolution techniques, such as Multiple Signal Classification.**

Keywords*— *uterine contraction interference signal, linearisation, MUSIC, bispectrum, bicoherence

I. INTRODUCTION

The non-linear transabdominally-measured ECG signals are contaminated by non-linear labour Uterine Contraction Interference Signals (UCIS) and some non-linear noise [1]. One way of improving the signal quality and reduce noise is by the use of linearization. Linearisation is performed by means of synthesising the non-linearity of all ECG signals into their linear, quadratic and cubic components using adaptive LMS- or LMF-based Volterra filters [2]. Only the linear components are retained for further processing [3]. This minimises non-linear sourced distortions and improves the fetal heart detection rates during labour [4]. The nature of the UCIS changes with the length of the observation data. For instance, if the UCIS is observed over 10,000 samples it can be modelled as deterministic, non-linear, and chaotic signals [1]. However, when observed over a 250-msec window, the UCIS may look just like noise. Hence, it is proposed to analyse the UCIS signal in order to characterise it before applying any further analysis, with the aim of linearising the signal, which will lead to simplified framework that will cater for the case of having bio-smart wireless ECG sensors with big data that needs special care in further processing. The paper is organised as follows; Section II summarises the data collection exercise. The UCIS short- and long-term statistics [5-9] will be discussed in sections III and IV, respectively. Section V summarises the UCIS spectral characteristics results. Summary is given in section VI.

II. DATA COLLECTION

ECG data were collected with consent from 30 healthy female volunteers. Data were sampled at 500 Hz. The data included maternal chest ECG signal, maternal transabdominal ECG signal, and a fetal scalp electrode ECG signal. The fetal scalp electrode was utilized, with the prior consent of the mother, when deemed necessary by the obstetrician. The patients were at the end of the gestation period, in trimester three, and all of them were around week 40 in labour. One of the ECG measurements was conducted using a wireless ECG sensor, employed with the LabChart of ADInstruments. The procedure of processing the data and obtaining the UCIS is described in [2, 4].

The UCIS data were obtained during the peak contraction time. This has been occurring, on average, every 10 minutes. It lasts, on average, for around 90 seconds. This portion of the data is the one utilized in this study in order to try to classify the UCIS data, and hence reduce its presence in the transbdominal ECG data to improve the detection ratio of transdabdominal fetal heartbeats during labour, with the fetal scalp electrode data utilized as the gold standard for verification.

III. UCIS SHORT-TERM STATISTICS

The modified covariance (correlation) matrix, $\mathbf{I}_{noise}$, of the UCIS data was established progressively in time from the measured contraction signal which is segmented into small portions of 250 sec each. The Hinich Test for Gaussianity was applied to the $\mathbf{I}_{noise}$ matrix. The matrix does not satisfy the hypothesis of Gaussianity at a confidence level of 95%. The Gaussianity parameter, S-Gauss, was calculated to be 163.5 which is different from 0 for the Gaussianity assumption to be valid. So it is assumed that the $\mathbf{I}_{noise}$ matrix is non-Gaussian.

The modified covariance matrix of the UCIS, $\mathbf{I}_{noise}$ matrix, is correlated because its off diagonal elements are non-zero. The statistics of the $\mathbf{I}_{noise}$ matrix are calculated from the

978-1-5090-4568-6/16/$31.00 ©2016 IEEE

following equations for the variance, skewness, and kurtosis, which are defined, respectively, as

$$\gamma_2^x \underline{\underline{\nabla}} c_2^x(0) = \frac{1}{2\pi}\int_{-\pi}^{\pi} C_2^x(\omega).d\omega \tag{1}$$

$$\gamma_3^x \underline{\underline{\nabla}} c_3^x(0,0) = \frac{1}{(2\pi)^2}\int_{-\pi-\pi}^{\pi\ \pi} C_3^x(\omega_1,\omega_2).d\omega_1.d\omega_2 \tag{2}$$

$$\gamma_4^x \underline{\underline{\nabla}} c_4^x(0,0,0) = \frac{1}{(2\pi)^3}\int_{-\pi-\pi-\pi}^{\pi\ \pi\ \pi} C_4^x(\omega_1,\omega_2,\omega_3).d\omega_1.d\omega_2.d\omega_3 \tag{3}$$

The variance of $\mathbf{I}_{noise}$ equals 0.957, the skewness equals 1.321, and the Kurtosis equals 2.637. The skewness and kurtosis are calculated from the third- and fourth-order statistics of the $\mathbf{I}_{noise}$ which confirms that $\mathbf{I}_{noise}$ is non-Gaussian because its higher-order statistics are not equal to zero.

The statistics of $\mathbf{I}_{noise}$ are different from the Uniform and Laplace noise which do not support third-order statistics because they are symmetrically distributed. They are also different from the Exponential and Rayleigh because its second, third- and fourth-order statistics are not related by one constant, e.g.,λ, α.

IV. UCIS Long-Term Statistics

The UCIS signal, when considered over a sufficiently long data sample of length 10,000 or more [1], is deterministic, chaotic, and multi-fractal. Essentially, the multi-fractility is indicative of normality in this case. Based on the Hinich linearity test and the Hurst component analysis test [10] which will now be described.

A. The Hinich linearity test

The test is based on the observation that for a linear process the skewness will be constant [5]. In the Hinich linearity test, the inter-quartile range of the estimated bicoherence squared is computed; a quantity, Λ, proportional to the mean value of the bicoherence squared is also computed; the theoretical inter-quartile range of a chi-square random variable with two degrees of freedom and non-centrality parameter, Λ, is then computed. The linearity hypothesis should be rejected if the estimated and theoretical inter-quartile ranges are very different from one another. The non-centrality parameter is

$$\Lambda = \frac{2N}{\left(1+\rho^{-1}\right)^3}\Gamma_s, \tag{4}$$

where Λ is the non-centrality parameter, N is the number of samples, ρ is the signal-to-noise ratio, and Γ_s is the skewness of the signal. The estimated and theoretical inter-quartile ranges are 268.91 and 42.59, respectively. Hence, the non-linearity hypothesis was accepted.

B. The Chaoticity Hurst component test

The test is based on the observation that multi-fractal signals can be decomposed into many subsets characterised by different local Hurst exponents, h, which quantify the local singular behaviour and relate to the local scaling of the signal. The local value of h is extracted using the Wavelet theory. The local exponent, h, is evaluated through the modulus of the maxima values of the wavelet transform at each point of the signal. A function $Z_q(a)$ is defined as the sum of the qth powers of the local maxima of the modulus of the wavelet transform coefficients at scale a. The scaling of that partitioning function, $Z_q(a)$, is estimated. For small scales, the partitioning function $Z_q(a)$ scales is expected to be as a power law,

$$Z_q(a) = a^{t(q)}. \tag{5}$$

For certain values of q, the exponents t(q) have familiar meanings. In particular, t(2) is related to the scaling exponent of the Fourier power spectra,

$$S(f) \cong \frac{1}{f^b}, as\ b = 2 + t(2). \tag{6}$$

For positive q, $Z_q(a)$ reflects the scaling of the large fluctuations and strong singularities, whereas for negative q, $Z_q(a)$ reflects the scaling of the small fluctuations and weak singularities. For multi-fractal signals, t(q) is a non-linear function:

$$t(q) = q\,.h - D\,(h), \tag{7}$$

where

$$h = \frac{dt}{dq} \tag{8}$$

is not constant. The fractal dimension D(h) is related to t(q) through a Legendre transform:

$$D\,(h) = q\,.h - t(q). \tag{9}$$

The local Hurst exponents, h, quantify the local singular behaviour and thus relate to the local scaling of the time series.

Using the 10,000 samples of the UCIS, the partitioning function was calculated for scales a > 8 and for values of q ranges from -5 to 5. It was found that t(q) is a non-linear function of q; also D(h) has non-zero values for a broad range of the local Hurst exponents, h, which indicates that the corresponding UCIS is a multi-fractal signal [1].

The range of scaling exponents ($0 < h < 0.4$) with non-zero fractal dimension D(h) indicates that the fluctuations in the

978-1-5090-4568-6/16/$31.00 ©2016 IEEE

UCIS exhibit anti-correlated behaviour (h = 1/2 corresponds to uncorrelated behaviour; h > 1/2 corresponds to correlated behaviour). Hence, the UCS is a deterministic, non-linear, and chaotic signal.

V. The UCIS Spectral Characteristics

The UCIS broad spectrum will now be briefly addressed. It has been found from previous research studies [3, 11] that, the spectrum of the UCIS may include comparatively strong narrowband spectral components centred around 5 Hz, 30 Hz, 45 Hz, 60 Hz, and 90 Hz in addition to some broadband components. Figure 1 depicts UCIS spectral characteristics before and after linearisation using a third-order Volterra synthesiser. This included calculating the linear, quadratic, and cubic parts, and retaining only the linear part. The spectral peaks were calculated using the power spectrum (top) and the Kaiser-Windowed super-resolution Multiple Signal Classification (bottom) which shows sharper peaks. Both parts reveal frequency components of the UCIS signal that overlaps with the fetal principal spectral peak of 30 Hz. This shows the difficulty faced when trying to resolve the signals in the frequency domain. The UCIS signal is also overlapping with the ECG signal in the time domain. This is what led to the attempt to resolve the signals using the signal and noise subspace techniques utilizing the orthogonalisation of their eigenvalues and eigenvectors obtained from the modified covariance matrix.

Figure 2 depicts the effect of linearisation on the UCIS's bicoherence squared. Linearisation has resulted in an average reduction of about 9 dB in spectral peaks at frequency pairs of (32 Hz,18 Hz), (32 Hz,48 Hz), and (48 Hz,32 Hz). Reducing the nonlinearity and utilizing a linear model simplifies the analysis and makes it easier to using the modified covariance matrix to steer the eigenvectors into orthogonalisation where the UCIS would have eigenvectors orthogonal to both the maternal and fetal eigenvectors. The latter, although overlapping 10% of the time in the time domain, but they could be separated in the frequency domain employing their respective principal spectral peaks. This is because the maternal spectral peak is centred around 17 Hz and the fetal peak is centred around 30 Hz.

The aforementioned UCIS spectral peaks are strongly overlapping with the fetal frequency pairs depicted in Figure 3 for both (a) transabdominally-measure and (b) fetal scalp measured, at (30 Hz, 7 Hz), (30 Hz, 18 Hz), and (30 Hz, 26 Hz).

VI. Conclusion

In this paper the Uterine Contraction Interference Signal (UCIS) of a transabdominal ECG signal was obtained, isolated, characterised and processed. The short-term data analysis reveals that the data is nob-Gaussian. The long-term data analysis using Hinich test suggests that the data is non-linear. Furthermore, the chaoticity Hurst component test leads to the fact that the data is deterministic and chaotic. Spectral analysis of the data has been performed and contrasted for the cases of raw data with the linearised data. This showed frequency domain overlapping between the UCIS and the fetal respective principal spectral peaks. This led to the proposed orthogonalisation of the eigenvectors of the UCIS in one hand and those of the maternal and fetal eigenvectors on the other. This would eliminate the undesired effect of the UCIS on the combined signal. Hence, it would be possible to improve the fetal heartbeat detection by employing a super-resolution Multiple Signal Classification routine since the principal spectral peaks of the mother and fetal are not overlapping, even though t maternal and fetal R peaks of their respective QRSs often overlap, with an overage of 10% occurrence throughout the whole data records.

References

[1] M. S. Risk, W. Zgallai, E. R. Carson, K. T. V.Grattan, A. MacLean, and P. Hardiman, "Non-linear dynamic tools for characterising abdominal Electromyographic signals before and during labour," Transactions of the Institute of Measurement and Control, Vol. 22, pp. 243-270, 2000.

[2] W. A. Zgallai, "MUSIC Incorporating Uterine contraction in Non-invasive Fetal Heartbeat Detection", Second International Conference on Signal and Image Processing, D. Wyld et al., Eds, pp. 191-198, ISBN 978-1-921987-46-5, AIRCC, UAE, 22-23/1/2016. https://arxiv.org/submit/1478402/view

[3] M. S. Rizk, W. Zgallai E. R. Carson, K. T. V. Grattan, P. Hardiman, P. Thompson and A. Maclean, "Modified MUSIC Pseudospectral Analysis Reveals Common Uterus and Fetal Heart Resonances during Labour Contractions", the 22nd International Conference of the IEEE Engineering in Medicine and Biology Society, EMB2000, USA, 23-28/7/2000.

[4] W. A. Zgallai, "MUSIC fetal heartbeat detection during uterine contraction, "The International Conference on Biomedical Engineering and Environmental Technology, (BMEET2015) London, 21-22/3/2015.

[5] M. J. Hinich, "Test for Gaussianity and linearity of a stationary time series," Journal of time series analysis, vol. 3, No. 3, pp. 169-176, 1982.

[6] H. E. Hurst, "Long-term storage capacity of reservoirs," Transactions of the American Society of Civil Engineers, Vol. 116, pp. 770-808, 1951.

[7] T. Vicsek, Fractal Growth Phenomena, 2nd edition, World Scientific, Singapore, 1993.

[8] H. Takayasu, Fractals in the physical sciences, Manchester University Press, UK, 1997.

[9] H. E. Stanley, in Fractals and disordered systems, 2nd edition, A. Bunde and S. Halvin, eds., pp. 1 – 68, Springer, Brerlin, 1996.

[10] P. Ch. Ivanov, et al., "Multifractality in human heartbeat dynamics", Nature, vol. 399, pp. 461-465, 3 June 1999.

[11] M. S. Rizk, W. Zgallai, A. MacLean, and E. R. Carson, "Multi-fractility in labour contraction dynamics," The 2nd Joint Conference of the IEEE Engineering in Medicine and Biology Society and the Biomedical Engineering Society,23-26/10/2002, Houston, Texas, USA.

978-1-5090-4568-6/16/$31.00 ©2016 IEEE

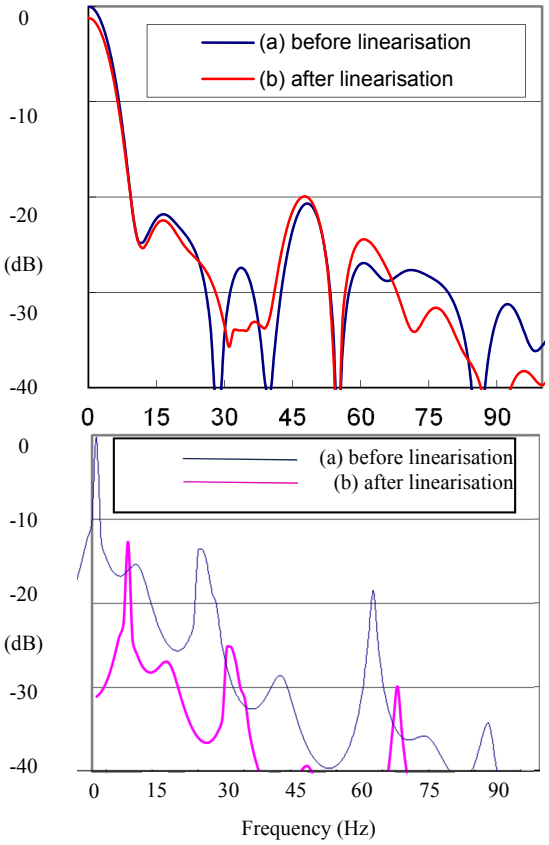

Figure 1: *Spectral properties of a uterine contraction plus noise segment. (top) Power spectrum (in dB) and (bottom) Kaiser shaped weighted MUSIC pseudo-spectral peaks (in dB) (a) before and (b) after linearisation using only the linear part of the output of a third-order Volterra synthesiser. The output consists of the linear, quadratic, and cubic parts of the transabdominally-measured ECG 250 msec segment, and free of both P-waves and QRS-complexes. The Welch averaged periodogram method is used to calculate the power spectrum. The MUSIC model order is 11 and 4 for the signal and noise subspaces, respectively. Optimised Kaiser weighting coefficients were used. Volterra synthesiser parameters are: filter length = 6, delay = 2, step-size parameters =0.001, 0.0001, 0.00001, for linear, quadratic and cubic parts, respectively. Code: 9-67.*

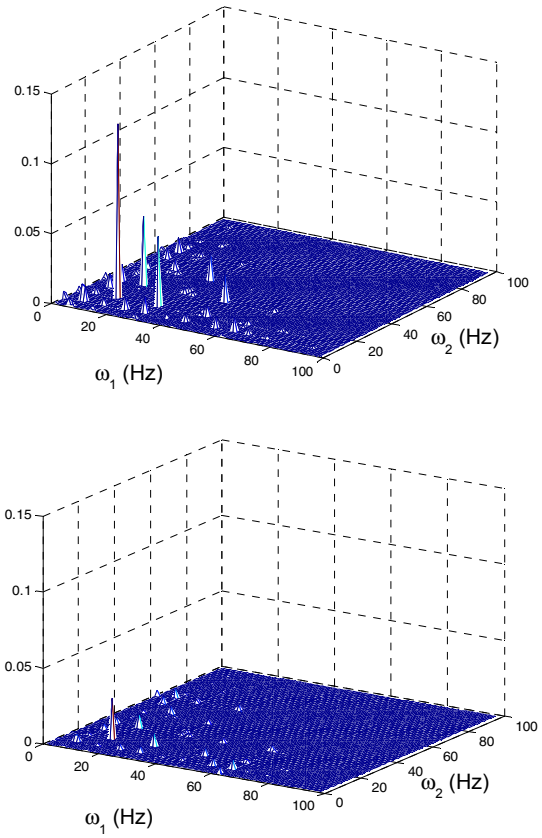

Figure 2: *The bicoherence squared (Kaiser shaped window) of the transabdominally-measured ECG 250 msec segment which is free from both the P-waves and the QRS-complexes (top) before and (bottom) after linearisation using a third-order Volterra synthesiser. Retaining only the linear part results in a significant reduction in artefact. The direct method was used to calculate the bispectrum and then normalised with the Welch averaged periodogram to obtain the bicoherence squared. The Volterra synthesiser parameters are: filter length = 6, delay = 2, step-size parameters =0.001, 0.0001, 0.00001, for linear, quadratic and cubic parts, respectively. Code: 9-67.*

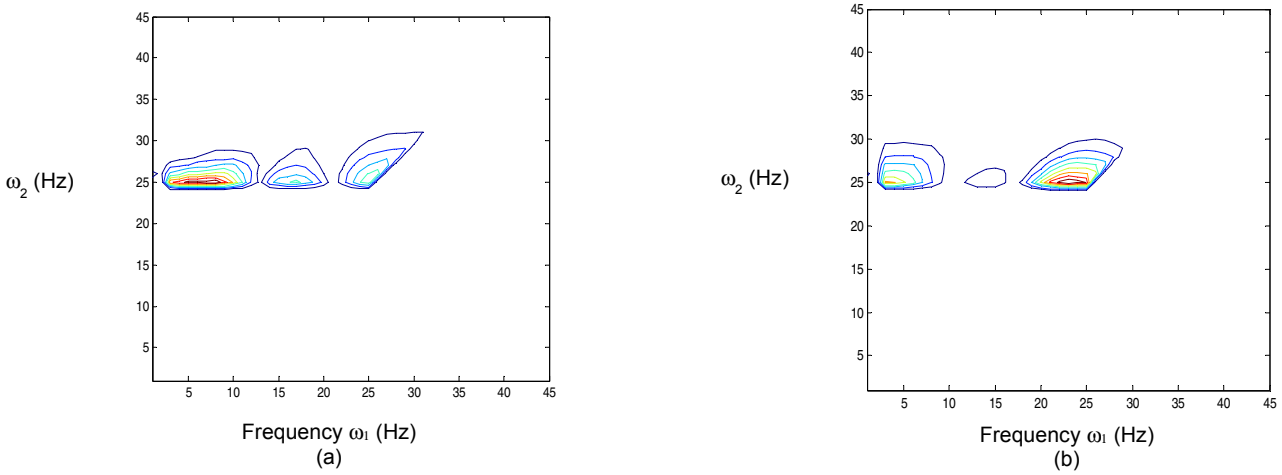

Figure 3: *(a.) Bispectral contours for the transabdominally-measured ECG 250 msec segment containing the first fetal heartbeat with maternal contribution. (b) Bispectral contours for the synchronised fetal scalp electrode ECG. The bispectrum is calculated using the direct method with a Kaiser window applied to the 250 msec segment.*